Journal of Materials Chemistry

Cite this: *J. Mater. Chem.*, 2011, **21**, 16077

www.rsc.org/materials

PAPER

Characterization and drug release behavior of chip-like amphiphilic chitosan–silica hybrid hydrogel for electrically modulated release of ethosuximide: an *in vitro* study†

Wei-Chen Huang, Tai-Jung Lee, Chi-Sheng Hsiao, San-Yuan Chen* and Dean-Mo Liu*

Received 27th May 2011, Accepted 9th August 2011
DOI: 10.1039/c1jm12376a

The hydrogel response under environmental induction often decreases with time because of the mechanical weakness of polymeric hydrogels. Therefore, to reinforce the conventional hydrogels with improved responsiveness and service performance to an external stimulus, a hybrid hydrogel consisting of an amphiphilic chitosan and inorganic silica with a minimal concentration of organic cross-linker was made in order to ascertain the biocompatibility of resulting hydrogels and improve stimulus-induced responsiveness. The hybrid hydrogels generally illustrated a rapid drug (ethosuximide, ESM) release profile over a time period of less than 60 minutes. However, after assembling the hybrid hydrogels into a chip-like device, the sandwiched hybrid showed, under a number of applied DC voltages, a variety of release profiles from a burst-like to slow-elution pattern. A release mechanism was proposed and can be successfully explained as a result of combined effects of electrophoretic and electroosmotic operations. Kinetic analysis indicated that the ESM released from the chip-like device is essentially a shuttle between the swelling-controlled pattern and the diffusion-controlled mechanism, depending on the chemical compositions that were used to prepare the hybrid hydrogels under a given DC electrical field. The hybrid hydrogel chip-like device designed in this work has experimentally proved its technical potential as an electrically responsive drug delivery system to meet various biomedical demands.

1. Introduction

The demands for response-induced features of a drug delivery system have been most interesting and are driving its future market development due to a number of factors particularly involving the increased amount of aged population.[1] Therefore, an environmentally sensitive drug delivery system is required and designed, including stimulus-responsive real-time controlled drug release, with on-demand dosage capability. Drug delivery systems can be controlled by applying an external stimulus including electrical field, magnetic field, ultrasonic waves, light, pressure, pH and biomolecules, upon which the drug is eluted with a pre-designed pattern from the system to the diseased host to minimize life-threatening occurrences.[2–6]

Use of an environmentally responsive hydrogel as a reservoir to deliver therapeutic substances has received wide attention over recent decades.[7,8] However, the mechanical weakness of polymeric hydrogels renders long-term application more challenging, for instance, structural collapse or degradation of a given hydrogel under environmentally induced (mostly, electric field) mechanical deformation may occur. Relaxation of the deformed hydrogel when removing the induced field may also retard the efficiency of the subsequent release of the drug, reducing therapeutic efficacy to a certain extent.

Hydrogels sensitive to electric current are usually made of polyelectrolytes, such as pH-sensitive hydrogels. Under the influence of an electric field, electro-responsive hydrogels generally deswell or bend.[9] Since volume changes of many responsive hydrogels are usually diffusion-controlled,[10–12] the deswelling equilibrium can only be reached slowly, *i.e.*, hydrogel response to an electric stimulus is slow. The extent of the hydrogel deswelling increases with the magnitude of the electric field, but is not linearly proportional to it. Gong *et al.*[13] and Budtova *et al.*[14] have shown that the extent of deswelling depends on the amount of charge transported through the hydrogels, rather than on the voltage applied. Three main mechanisms of electro-induced gel deswelling have been suggested, which include: (1) a stress gradient developed in the hydrogel, (2) changes in local pH around the electrodes and (3) electroosmosis of water coupled to electrophoresis. The mechanical response of polyelectrolyte hydrogels to an applied electric field can be used to control drug release from these gels. To a large extent, the effects of electrical stimulation on drug release depend on the

Department of Materials Sciences and Engineering, National Chiao Tung University, Hsinchu, 30010, Taiwan. E-mail: sanyuanchen@mail.nctu.edu.tw; deanmo_liu@yahoo.ca

† Electronic supplementary information (ESI) available. See DOI: 10.1039/c1jm12376a

mechanisms by which the hydrogel responds to the stimulus and any interactions between the drug and the hydrogel network. Ramanathan and Block[11] first used chitosan as matrices for electrically modulated drug delivery and found that gel syneresis was pronounced, particularly at higher milliamperage (mA) for chitosan gels with lower degrees of acetylation. In addition, the IPN system can be a promising candidate to meet many requirements because it can induce quite strong mechanical properties. Therefore, chitosan/polyallylamine IPN,[15] poly(vinyl alcohol)/chitosan IPN,[16] chitosan/poly (diallyldimethylammonium chloride) semi-IPN[17] and chitosan/hyaluronic acid complex[18] were synthesized and characterized for their electrical sensitivity.

However, the magnitude of the hydrogel response under environmental induction (mostly, electric field) often decreased with time because of the mechanical weakness of polymeric hydrogels, for instance, structural collapse or degradation of a given hydrogel. Increasing addition of a chemical cross-linker may achieve better performance, however, deteriorating biocompatibility of the resulting hydrogels. Therefore, to reinforce the conventional hydrogels with improved responsiveness and service performance to the external stimulus, an attempt of incorporating a suitable amount of inorganic component together with a minimal concentration of organic cross-linker was made in order to ascertain the biocompatibility of resulting hydrogels and improve stimulus-induced responsiveness. In this work, an amphiphilic chitosan which was biocompatible, non-toxic, non-irritable, and moisturized as described in our previous publications was employed as the organic matrix.[19] This modified chitosan was further hybridized with an inorganic silica sol and a small amount of cross-linking agent to form a hybrid matrix aimed to be employed as a drug delivery system. Ethosuximide (ESM) is a water-soluble drug and a proposed T-type Ca^{2+} channel blocker. It has been successfully employed to eliminate partial seizures and used as the first-choice therapeutic agent to ameliorate clinical spike-wave discharge (SWD) occurrences. As epilepsy seizure occurred, an abnormal electrical discharge was generated, which needs the drug to be rapidly released for prohibiting the seizure. Therefore, ESM was used in this investigation as the model drug. The resulting hybrid hydrogels were employed as a drug reservoir to study the drug release behavior for an electrically responsive drug delivery system. The results show that the hybrid hydrogel chip-like structure designed in this work has demonstrated a number of electrically modulated drug release profiles *in vitro* ranging from burst-like to slow-elution patterns.

2. Experimental procedures

2-1 Synthesis of carboxymethyl-hexanoyl chitosan

The synthesis of amphiphilic carboxymethyl-hexanoyl chitosan (CHC) has been detailed in a previous report.[19] Briefly, 5 g of chitosan (M_w =215 000 g mol^{-1}, deacetylation degree = 85–90%, supplied from Aldrich-Sigma) was suspended in 2-propanol (50 ml) at room temperature while being stirred for 30 min. The resulting suspension was gently mixed with 12.5 ml NaOH solution. The mixture containing NaOH of 13.3 M was mixed with 25 g of chloroacetic acid to prepare a carboxymethyl chitosan sample with a high degree of carboxymethyl substitution. Two grams of dried sample was dissolved in distilled water (50 ml) and stirred for 24 h. The resulting solutions were mixed with methanol (50 ml), followed by adding hexanoyl anhydride at a concentration of 0.5 M to the CHC samples. Upon substitution, from NMR analysis, 48% of amine groups were substituted by acetyl-hexanoyl groups and 50% of the hydroxyl groups were replaced by carboxymethyl groups. Hence this made the final CHC more soluble in physiological pH and our study revealed, after the CHC dissolved in DI water (pH = 6.6), forming a slightly acidic pH (5–5.5) solution. This indicated that deprotonation of the modified CHC polymer in DI water had occurred and the resulting CHC nanocapsules, with a negatively charged ζ-potential, had been formed. These important chemical parameters such as the degree of substitution (*i.e.*, values of 0.5 and 0.48) and residual free amino groups have readily been studied in previous publications.[19] After a 12 h reaction, the resulting solutions were collected by a dialysis membrane (Sigma Chemical Company, USA) using ethanol solution (25% v/v) for 24 h, till a dried powder was obtained after drying at 50 °C overnight.

2-2 Preparation of CHC–silica hybrid hydrogels

The CHC–silica hybrid hydrogels were prepared through mixing three chemical solutions: (1) 1.3% w/v CHC solution by suspending the above-mentioned CHC samples in deionized water at 25 °C for 24 hours; (2) 1% w/v GP (genipin, Challenge Bioproducts Co., Ltd, Taiwan) solution which is prepared by dissolving GP powders in deionized water stirring for 2 hours at 50 °C to ensure that GP was fully dissolved; and (3) acid-hydrolyzed tetraethoxysilane (TEOS) solution, by mixing TEOS with ethanol and HCl acidified H_2O (0.1 M) with different weight ratios ([TEOS] : [H_2O] : [Ethanol] = 1 : 5 : 7, 2 : 5 : 7, and 1 : 10 : 14 separately). The structural illustration of the synthetic procedure is presented in the ESI of Fig. S1†. The GP and TEOS solutions with different weight ratios were added to the CHC solution stirred for 30 minutes, followed by incubating at 50 °C for 2 days. Thus, the genipin-cross-linked CHC–silica hybrid hydrogels were formed and designated as GP*x*TEOS*y*, where the symbols *x* and *y* represent the weight ratios (in percentage) in the dried hydrogel. The synthetic parameters of hybrid hydrogels are listed in Table 1.

2-3 Characterization

The hybrid hydrogel samples were obtained *via* casting and drying the final solution mixture at 50 °C in a Petri-dish with

Table 1 The synthesis parameters of CHC–TEOS hybrid hydrogels designated as GP*x*TEOS*y*, where the symbols *x* and *y* represent the weight ratios in the dried hybrid hydrogel

Hybrid hydrogel	1.3% w/v $CHC_{(sol)}$/g	1% w/v $GP_{(sol)}$/g	TEOS/g
GP0TEOS54	2	0	0.03
GP0.5TEOS54	2	0.03	0.03
GP1TEOS54	2	0.06	0.03
GP1.5TEOS54	2	0.12	0.03
GP1.5TEOS0	2	0.12	0
GP1.5TEOS27	2	0.12	0.018
GP1.5TEOS54	2	0.12	0.03
GP1.5TEOS70	2	0.12	0.045

a size of 3.0 cm in diameter. The average thickness and the average weight of the obtained dried hydrogels were about 0.10 mm and 0.3 g, respectively.

The appearance and morphology of the hybrid hydrogels were examined by using optical microscopy and scanning electron microscopy (S6700, JEOL, Japan) respectively. Samples, named as GP0TEOS54, GP0.5TEOS54, GP1TEOS54, and GP1.5TEOS54, were characterized by UV spectroscopy (Evolution 300, UV-Vis), where the resulting spectra show different absorption wavelengths, representing variation in the cross-linked density. Moreover, the dynamic weight loss test for those samples, *i.e.*, GP1.5TEOS0, GP1.5TEOS27, GP1.5TEOS54, and GP1.5TEOS70, was conducted through a DuPont 2050 thermogravimetric analyzer which in the meantime is able to investigate the degree of interweaving of the silica phase against the CHC phase. All tests were conducted in a flowing N_2 atmosphere (25 ml min^{-1}) using samples of 3–5 mg in weight over a temperature range of 30 °C to 500 °C at a scan rate of 10 °C min^{-1}.

The swelling ratio of the samples was estimated by measuring the change of sample weight before and after immersion in phosphate buffer solution. The procedure was repeated five times, until no further weight gain was detected. The swelling ratio was determined according to the following equation:

$$\text{Swelling ratio } (\%) = [(W_s - W_d)/W_d] \times 100$$

where W_s and W_d represent the weight of swollen and dried samples, respectively. All results are obtained by averaging five measurements. The measurement error is estimated <3%.

2-4 Drug delivery chip-like structure

The drug delivery chip-like structure was designed by casting the hybrid hydrogels into a transparent, plastic container. Fig. 1(a) illustrates schematically the preparation procedures of the chip-like structure. A transparent plastic container, made of poly (methyl methacrylate) (PMMA, YEONG-SHIN Co., LTD, Taiwan), has dimensions of 2 cm × 2 cm × 0.2 cm with a single small opening 0.2 mm in diameter on one side of the container, whilst the other three sides were mechanically sealed by the PMMA plates. The one with the small opening is designed as the outlet for drug elution. Two rectangle-shaped platinum plates (Pt, YEONG-SHIN Co., LTD, Taiwan, 4 cm × 2 cm × 0.1 mm in dimension) were placed at a constant distance of 0.5 mm with two parallel sides of the acrylic container as electrodes. After the ESM-loaded hybrid hydrogels, having dimensions of 4 cm × 2 cm × 0.3 mm, were inserted into the container, a chip-like structure was successfully prepared (Fig. 1(a) and (b)).

2-5 Drug release from hybrid hydrogel and the chip-like structure

The drug release test was carried out by mixing the hydrophilic anticonvulsant drug, ethosuximide (ESM), at a concentration of 15 mg ml^{-1}, into the CHC solutions. The drug was dissolved completely in the presence of the CHC-containing solution with a concentration of 1.5% by weight of the ESM. Then the genipin was added to synthesize the genipin-cross-linked CHC network which is originated from nucleophilic attack by the amino group of CHC toward the olefinic carbon atom at C-3 of deoxyloganin aglycone followed by the opening of the dihydropyran ring to form a heterocyclic amine. Subsequently, TEOS was subjected to acid-hydrolyzed treatment at pH = 1 to form acid-hydrolyzed TEOS which was added to the genipin-crosslinked CHC network to form a complete sol–gel reaction.

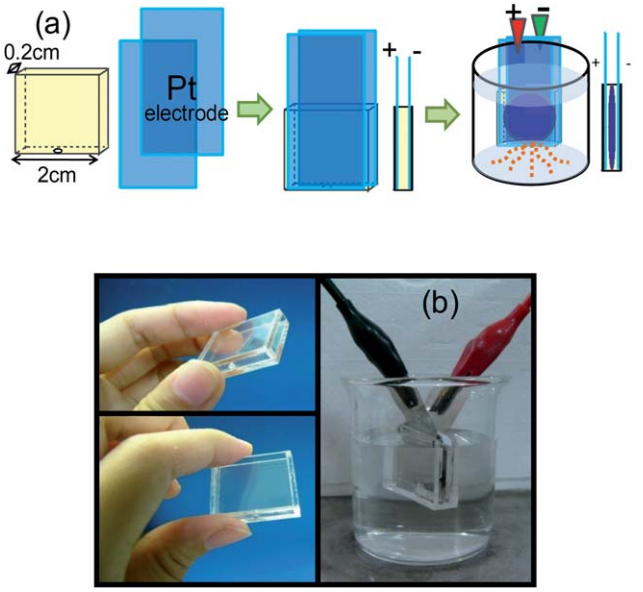

Fig. 1 (a) Procedures for the preparation of the drug delivery chip-like structure. (b) The setup of the hybrid hydrogel structure. An electrical field of different strength can be applied between the Pt electrodes in the sealed container for controlled release of drug molecules.

After vigorously stirring, the final ESM-containing CHC-TEOS solution was cast in a Petri dish and dried in an oven at 50 °C to form disk-shaped hydrogels according to the preparative procedures aforementioned. The resulting hydrogel disks were immersed into 50 ml distilled water and 2 ml of solution was extracted at pre-determined time intervals from the testing container and analyzed using a UV spectrophotometer (Evolution 300) at a specific wavelength $\lambda = 254$ nm. For the hybrid hydrogel chip-like structure, after the chip-like structure was immersed into a glass beaker containing a fixed amount of 50 ml distilled water, the swollen hybrid hydrogel was mechanically locked in the container with one small opening (0.5 mm in diameter) on one side of the structure. The chip was then exposed to an electric voltage generated by a DC power source over a range of 0 V, 15 V, 30 V, and 60 V across the Pt electrodes. ESM released from the hydrogel chip was monitored and analyzed under the same operation condition as that for the hybrid hydrogel aforementioned. In addition, in order to discuss about the contribution of ESM, Electrophoretic Light Scattering (ELS) was used for measuring the ζ-potential of ESM which was added into buffers with pH = 4, 7, and 10 as acid, neutral, and basic solutions, respectively.

3. Results and discussion

3-1 Morphological analysis

Fig. 2(a) shows the appearance of the hybrid hydrogels containing 54 wt% TEOS and various amounts of genipin (GP)

where, after incubation at 50 °C in an oven for 24 hours, the resulting hydrogels displayed a change from transparent, light-green to dark-green, while the GP concentration increased from 0% to 1.5%. The UV spectrum, Fig. 2(b), also demonstrates a change from featureless to a broad absorption peak between 560 and 650 nm when the GP concentration was increased from 0% to >1.5%. The increased intensity of the absorption peak over the range of 560–650 nm of the blue-light region also exactly reflected the color change of the hybrid hydrogels. These observations suggested the GP being reacted, displaying different colors; in general, the darker sample appearance is indicative of a higher cross-linked density *via* GP of the hydrogels.

TEOS was hydrolyzed and condensed to form a network structure which according to Liu *et al.*[20] may develop an interweaving network with CHC. The CHC hydrogels may then expect to form a network structure with TEOS as shown in Fig. 3(a) where no observable microscopic or macroscopic inhomogeneities were visually observed in the resulting hybrid hydrogels, indicating both the inorganic silica and CHC phases being distributed evenly throughout the samples. Meanwhile, with constant concentration of GP added, all the samples showed the same color appearance. Mechanical enhancement to the hybrid hydrogels can then be expected with higher TEOS content as demonstrated in Fig. S2 of the ESI†. The crosslinking mechanism of genipin with CHC showed that only the primary amine of CHC could be reacted with genipin through a C3 carbon attack. In this system, the final solution showed an acidic pH (pH value = 5–6.7) so that instead of forming hydrophobic $–COO^-$ groups, –COOH groups of CHC were demonstrated preferably to provide better hydrophilic CHC in our system. On the other hand, since carboxyl groups, –COOH, of the amphiphilic CHC molecules were extended toward the aqueous environment upon

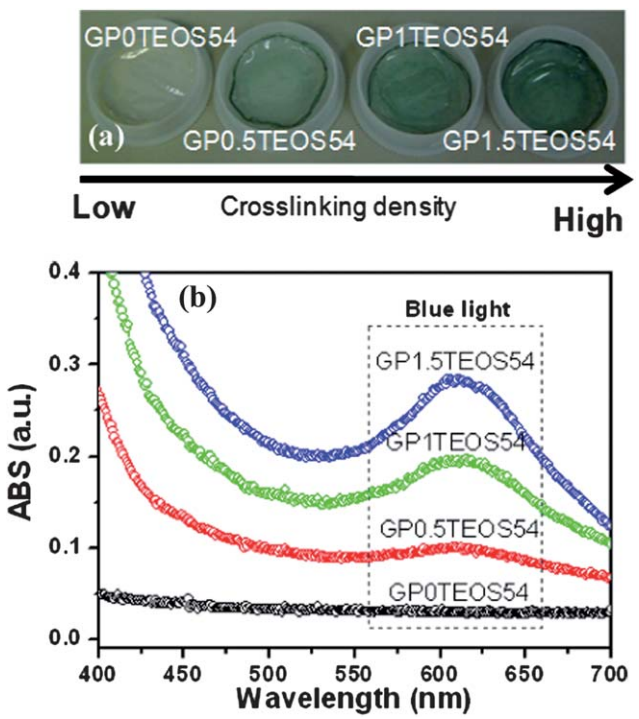

Fig. 2 (a) Optical photos of the hybrid hydrogels with different amounts of GP. (b) UV-Vis spectra of hybrid hydrogels of various compositions.

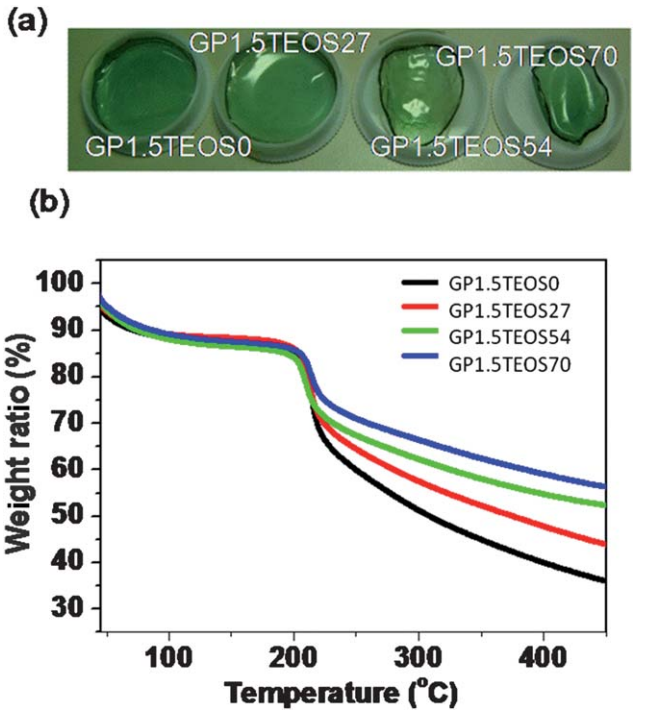

Fig. 3 (a) Optical microscopic photos of the hybrid hydrogels with different amounts (by weight percent) of TEOS and (b) the corresponding TGA profiles.

self-assembly, it is likely that hydrogen bonds are expected to develop between the –COOH groups and –OH groups from the hydrolyzed TEOS, allowing the formation of physical cross-linking between the CHC and silica components. Nevertheless, higher TEOS content imparts brittleness to the resulting hybrid hydrogels because of the formation of a rigid silicate network. Therefore, an optimal combination of both TEOS and GP has significance in reaching the resulting hybrid gel with better sustainability in applications.

3-2 Thermal analysis

Thermogravimetric analysis (TGA) of GP1.5TEOS0, GP1.5TEOS27, GP1.5TEOS54, and GP1.5TEOS70 shows that these four samples with different TEOS contents undergo a two-step thermal degradation process, Fig. 3(b). The first stage occurring at 30 °C–120 °C is due to evaporation of residual water and solvent which results in about 13.5% of weight loss. Above 200 °C, the CHC polymer started to decompose rapidly, following a long-tail degradation profile. As compared to Fig. S3† of pure CHC, the higher the amount of TEOS incorporated in the CHC matrix (while GP was kept constant), the lesser the extent, at the second stage, of the weight-loss profile observed, suggesting an improved structural stability due to the presence of higher silica content. Such a slow degradation profile, typically in regions >240 °C, suggested that the decomposition was considerably sluggish or inhibited through intermolecular cross-links. The cross-linking density was estimated by the weight loss (%) at 500 °C which was found to decrease in the order of GP1.5TEOS70 > GP1.5TEOS54 > GP1.5TEOS27 > GP1.5TEOS0. It is noted that the weight-loss difference enlarged

between the samples with increasing TEOS content under the same temperature, suggesting the contribution of cross-linking between the silica and CHC phases.

3-3 Swelling behavior

The swelling behaviors of the hybrid hydrogels with different amounts of GP and TEOS are illustrated in Fig. 4(a) and (b), respectively. The swelling profiles of GP0TEOS54 and GP1.5TEOS0 showed that both swollen hybrid hydrogels found it difficult to reach the swelling equilibrium but tended to collapse while immersed in water over a short period of time, *i.e.*, less than 30 minutes. In the absence of any crosslinking agents, the CHC was found to swell extensively till reaching a structural failure (collapse). Such structural failure probably results from dis-assembly of the CHC polymer chains as a result of dissolution and it is believed that the CHC polymer formed the micelle entities in water when reaching its critical micellization concentration (CMC) under ambient environment according to our previous study.[21] Similar structural dis-assembly also possibly occurred in the hybrid hydrogels using either 54% TEOS or 1.5% GP alone, as illustrated in Fig. 4(a) and (b), respectively. This structural collapse upon swelling may result from either the physical cross-link nature of the TEOS or insufficient cross-link reinforcement from GP. However, with the use of both TEOS and GP such as in samples GP0.5TEOS54, GP1TEOS54, GP1.5TEOS54, GP1.5TEOS27, GP1.5TEOS54, and GP1.5TEOS70, Fig. 4(a) and (b), prolonged swelling occurs till reaching an equilibrium state, albeit a final structural collapse occurred over a longer time period of >3 hours. The presence of both TEOS and GP provides a synergistic effect on improved structural integrity reducing dis-assembly upon swelling, compared to the cases of using TEOS or GP alone in the hybrid hydrogels.

However, an increase in the concentration of both GP and TEOS decreased the swelling ratio of the resulting hybrid hydrogels, indicating that the combined effects of both cross-linking and the silica phase constrained the swelling. The swelling behavior in Fig. 4(a) indicates that samples of GP0.5TEOS54, GP1TEOS54, and GP1.5TEOS54 (*i.e.*, hybrids with constant TEOS) show a decrease in swelling ratio with increasing GP concentration, 427%, 354%, and 269% for 0.5%, 1.0%, and 1.5%, respectively. Samples with constant GP, GP1.5TEOS27, GP1.5TEOS54, and GP1.5TEOS70, have a swelling ratio that decreased with increasing TEOS, from 550%, to 326%, and then to 300%. Reduced swelling of the hybrids suppressed the development of intermolecular voids (or mesh size) among the CHC chains (swelling effect), which, associated with the presence of silica barrier, affected a subsequent drug release behavior.

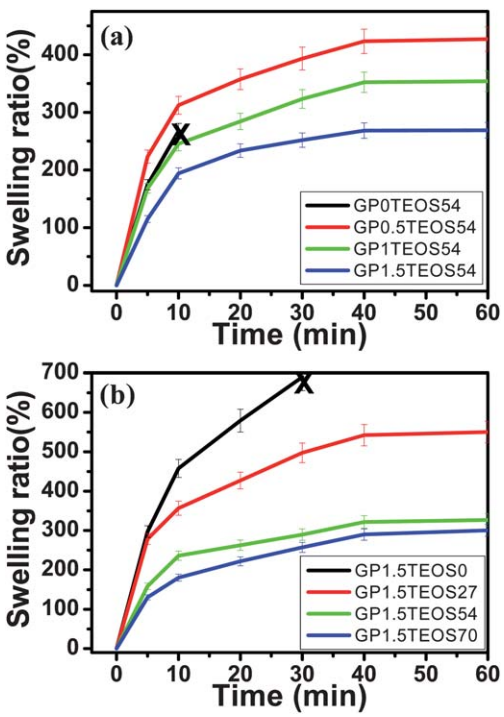

Fig. 4 Swelling behavior of the hybrid hydrogels with different contents of (a) GP of 0%, 0.5%, 1.0% and 1.5% (where TEOS is fixed at 54%) and (b) TEOS of 0%, 27%, 54%, and 70% (where GP is fixed at 1.5%), as a function of time.

3-4 Drug release behavior from the hybrid hydrogels

The *in vitro* release behavior of ESM from the CHC–TEOS hybrid hydrogels was measured over a 60 min period in deionized water, as shown in Fig. 5(a) and (b), for various amounts of GP (fixed amount of TEOS) and TEOS (fixed GP), respectively. The accumulated release in Fig. 5 represents the total normalized amount released from each hydrogel sample. The hybrid hydrogels with either TEOS or GP alone illustrated a rapid release where the ESM was completely eluted within 15 minutes because of the lack of sufficient cross-linking density (without either GP or TEOS) and rigidity (no TEOS), which caused an enormous structural dilation upon swelling (for pure CHC hydrogel, a swelling ratio of as much as 8 times in volume was detected). Therefore, after 5 minutes of eluting, an amount as large as 50–70% of the drug was eluted. However, hybrid hydrogels with combined TEOS and GP, such as GP0.5TEOS54, GP1TEOS54, GP1.5TEOS54, GP1.5TEOS27, GP1.5TEOS54, and GP1.5TEOS70, exhibited slower release profiles, and this was especially pronounced for the hybrids with higher GP and TEOS. The slower release profile for the hybrids with combined cross-linking natures may be interpreted as a combination of having a higher cross-link density due to higher GP and incorporation of sufficient amount of silica phase, where the former leads to a smaller intermolecular voids since the CHC chain mobility is extensively prohibited, while the latter may increase the diffusion path (tortuosity), throughout the hybrid networks, resulting in a slower ESM diffusion. Hence, although an early-phase burst release, up to 50–70% of ESM, was detected for all those hybrid hydrogels, Fig. 5(a) and (b), a number of drug release profiles can be tuned to a certain extent at a later stage of release through the manipulation of the chemical composition of the hybrid hydrogels. However, when exposed to an electrical field, release profiles for all these hybrid hydrogels were largely inhibited and the relevant drug release behavior (to be discussed in forthcoming analysis) is determined *via* the assembled chip-type device rather than the hydrogel itself, under electrical-field application. The purpose of such a design is intended for

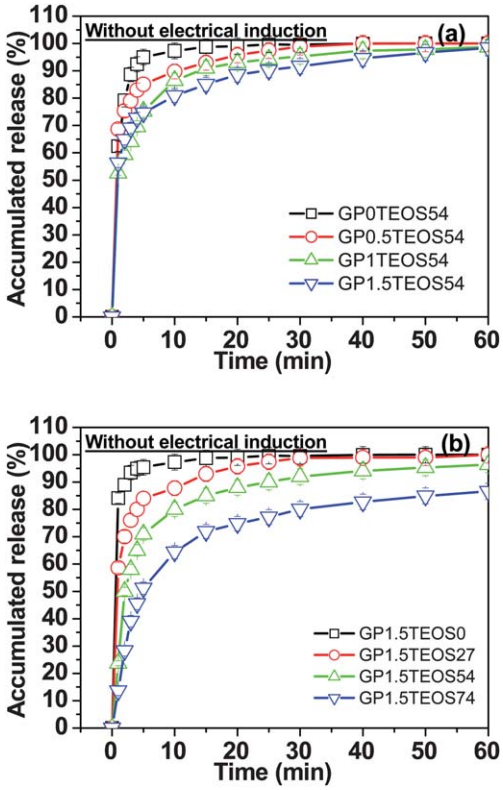

Fig. 5 *In vitro* release of ESM from the hybrid hydrogels with different amounts of (a) GP of 0%, 0.5%, 1.0%, and 1.5% (under constant TEOS) and (b) TEOS of 0%, 27%, 54%, and 70% (under constant GP) in the absence of electrical-field application. The accumulated release represents the total normalized amount released from each hydrogel sample.

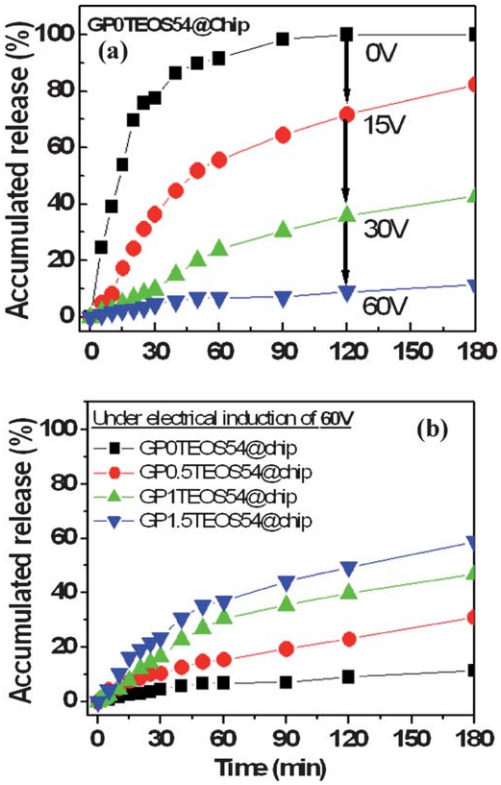

Fig. 6 (a) The ESM release profiles from GP0TEOS54 when the applied DC electric field was operated as 0 V, 15 V, 30 V, and 60 V. (b) The release profiles with different GP contents under electrical operation of 60 V.

a subsequent implantable electrically modulated drug delivery application for chronic disease treatment *in vivo*.

3-5 Drug release behavior of the hydrogel chip under electric field

3-5-1 Effect of GP. Fig. 6(a) shows the *in vitro* release of ESM from the GP0TEOS54 chip under an applied electric field of different DC voltages from 0 V to 60 V. ESM was completely depleted over a time period of 120 minutes under zero voltage. Compared with Fig. 5(a), the much slower release profile for the chip is a result of the small opening, which is the only outlet for drug release to the environment, whilst the hybrid hydrogel afore-mentioned exposed all available surfaces to the environment. Meanwhile, since the swelling of the hybrids sandwiched in the container is heavily restricted (estimated only to reach 80% of the equivalent swelling ratio given in Fig. 4(a)), a considerable reduction of intermolecular size from the fully swollen state within the hybrid network is expected to render a much slower release behavior. Increasing applied voltages to 15 V, 30 V, and 60 V demonstrated a continuing decrease in the accumulated release amount, to below 15%, at 60 V over a time period of 180 minutes. Such an electrically modulated ESM release profile from the hybrid hydrogels can be considered a result of both electrophoretic and electroosmotic actions interplaying between the hybrid network and ESM.

The chemical structure of ESM has a chiral framework containing a five-membered ring, with two negatively charged carbonyl oxygen atoms with a ring nitrogen between them and one asymmetric carbon atom, as shown in Fig. 7. Normally, it is more stable for ESM to perform with a dehydrogenated structure. It means that the electron resonance between the two carbonyl oxygen atoms and the dehydrogenated nitrogen atom will give rise to a negatively charged ESM, which has been verified by Electrophoretic Light Scattering where its ζ-potential is given in Table 2.

Hence, upon application of an electrical stimulus, the H^+ ion, located at the nitrogen of ESM, preferred to escape and become reduced at the cathode surface. In the meantime, the ESM molecules, which lost protons, should display electrophoretic movement to the anode. On the other hand, the immobile positive charges on the CHC polymer chain may also exert an attractive force upon the negatively charged ESM as a result of the electrolysis in the presence of electric voltage.

However, with an increase in GP, the release profiles under electrical stimulation at 60 V, in Fig. 6(b), show a faster release pattern. This observation is contrary to that in the absence of electrical stimulus, Fig. 5(a). This behavior can be explained by the fact that under acidic conditions, GP reacted with primary amino groups on chitosan to form heterocyclic amines, the reaction will reduce the positive charges on the polymer chains. It is reasonable to believe that the same reaction scenario can be reproduced in the CHC chain. On this basis, a higher cross-link density of the CHC chains with GP leads to a less positively

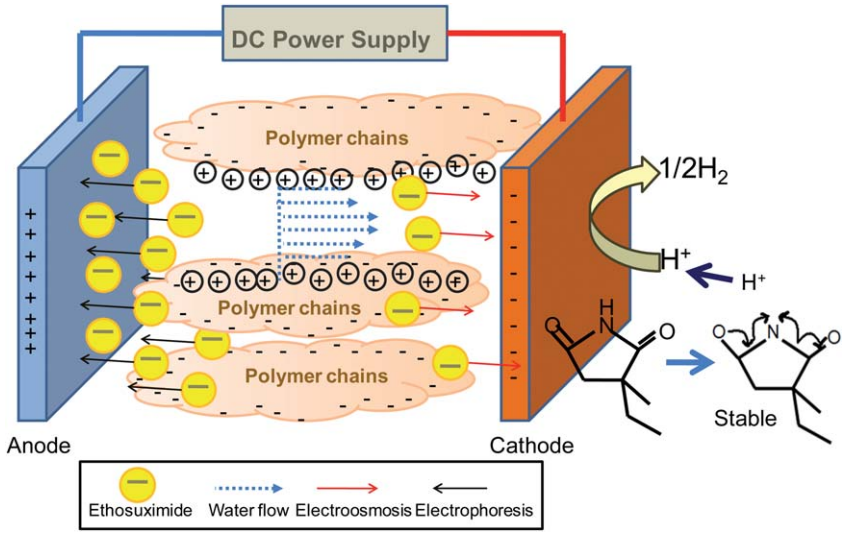

Fig. 7 The schematic drawing shows the influence of applied electrical voltage upon interactions between the ESM and CHC chains.

Table 2 ζ-Potential of ethosuximide at different pH values

pH values	ζ-Potential of ESM/mV
4	−9.82
7	−21.2
10	−45.7

charged CHC polymeric chain. Thus, the effect of electroosmosis, which also facilitates gel shrinkage, should be enhanced, as has been verified in ref. 22. Under such an action, the ESM is forced to move outward from the hybrids, leading to a faster release as the GP increased.

To investigate the release kinetics, kinetic parameters based on eqn (1) were employed and characterized in full:

$$\frac{M_t}{M_\infty} = kt^n \quad (1)$$

where M_t is the amount of drug released at time t, M_∞ is the amount of drug released at equilibrium state, k is a constant and n is the diffusion exponent related to the diffusion mechanism. Here, a UV spectrophotometer (Evolution 300) at a specific wavelength $\lambda = 254$ nm is used to analyze the measured absorption value of the amount of ESM released from the system. Hence, the unit of M_t in the system is Abs.

Lee *et al.*[23] distinguished three classes of diffusion according to the relative rates of diffusion and polymer relaxation. The first is Fickian diffusion ($n = 0.5$), in which the rate of diffusion is much smaller than the rate of relaxation. When the exponent n takes the value of 1.0, the drug release rate is independent of time (zero-order release kinetics). This indicates a swelling controlled mechanism (Case II transport). For most polymeric drug delivery systems, the values of n in eqn (1) are lying between 0.5 and 1, indicating that both the diffusion and relaxation rates are comparable in those drug delivery systems.

From the plot of ln (M_t/M) *versus* ln (t), kinetic parameters, n and K, were calculated, as listed in Table 3 where GP0.5TEOS54, GP1TEOS54, and GP1.5TEOS54 were also taken into account. The exponent n was strongly affected by the addition of GP, but also changed with applied voltage. The n value decreased from 0.744 to 0.561 as the GP increased from 0% to 1.5% in the absence of applied voltage (0 V). In this case, higher GP increased the cross-linking density, rendering the CHC chains less mobile upon swelling. This restricted the diffusion of ESM molecules, thus decreasing the diffusion exponent n.

On this basis, the drug release behavior shifted from a swelling-controlled towards a diffusion-controlled mechanism. However, electrical stimulus should deform the structure of the hydrogels, causing the n value of, for instance, GP0TEOS54 to increase from 0.744 to 0.797 under 15 V, then continuously increase from $n = 0.857$ (at $E = 30$ V) to $n = 0.897$ (at $E = 60$ V).

Upon the application of electrical voltage, the water molecules together with the ESM will be dragged toward the cathode by ion flow due to the gradient of ionic and osmotic pressure, forming electroosmosis flow. The two forces, electrophoresis and electroosmosis, which were in the direction parallel to the exposed surface, push ESM toward the sides of the chip and prevent the original downward force (*i.e.* orthogonal direction) of drug flow. This is the reason why the net release of the drug from the hybrid chips is largely restricted because of this electrical trapping effect. (Fig. 7).[22,24,25] With the increase of the applied voltage, those effects turned out to be more pronounced, giving rise to a much slower rate of drug release. Therefore, it can be concluded that the electric field provided a net force for ESM release due to the interactions of both electrophoresis and electroosmosis. Such combined actions caused the CHC chains to stretch but constrained the swelling to a certain extent, thus resulting in a swelling control release.

On the other hand, since the K value is represented as a constant of drug release rate, it was found that without electrical induction, the rate of drug release decreased with increasing GP. However, when the electric field was applied, smaller K values implied that the release rate was decreased. For example, when the voltage was applied above 30 V, K values of samples with GP contents as 0%, 0.5%, 1%, and 1.5%, were

Table 3 Kinetic constants K, and diffusion exponents n determined by linear regression of ESM release from the hybrid hydrogel chip, where the TEOS was fixed at 54% while GP increased from 0% to 1.5%

Sample label	Kinetic constant K				Release exponent n			
Applied voltage	0 V	15 V	30 V	60 V	0 V	15 V	30 V	60 V
GP0TEOS54	7.723	5.898	1.388	0.361	0.744	0.797	0.857	0.897
GP0.5TEOS54	6.455	5.912	2.001	0.680	0.670	0.815	0.868	0.935
GP1TEOS54	6.371	5.896	2.376	0.895	0.604	0.890	0.932	0.985
GP1.5TEOS54	6.082	6.076	4.235	0.970	0.561	0.928	0.942	0.993

found to be 1.38, 2.00, 2.38, and 4.24 (at $E = 30$ V), and 0.36, 0.68, 0.89, and 0.97 (at $E = 60$ V), respectively, smaller than those obtained in the absence of an electric field ($K = 7.72$, 6.46, 6.37, 6.08 at $E = 0$ V). Moreover, the external electric field boosted the release rate of hydrogels with more GP contents because the effect of electroosmosis would be enhanced. This result was consistent with the drug release behavior shown in release profiles of Fig. 6(a) and (b).

3-5-2 Effect of TEOS. Fig. 8(a) shows ESM release from the GP1.5TEOS0 chip when the electric field with different voltages was applied. The release profile showed a complete depletion of the drug over a time period of 120 minutes, which is much slower than those illustrated in Fig. 5(b), where almost 95% of drug was rapidly released out within 5 minutes. The obvious difference could be attributed to the swelling limitation resulting from the stereoscopic barrier of the assembled chip-like system. Since the chip was designed as a closed system with a tiny hole, the stereoscopic barrier limited the diffusion direction and rate of entering water so that the swelling of the hydrogel in the chip-like system was confined to be released arbitrarily. Hence the structural expanding and relaxing rate of network was controlled for releasing drug. Moreover, it also could be found that increase in the TEOS of the hybrids causes a decrease in the release profile. Such a change in ESM release behavior as a function of TEOS content is also similarly observed in the case of the hybrid hydrogels, whereas the swelling of the hybrids was largely restricted due to the presence of the non-swellable silicate phase and thus, reduced considerably the ESM release from the hybrid hydrogels and from the chips as well.

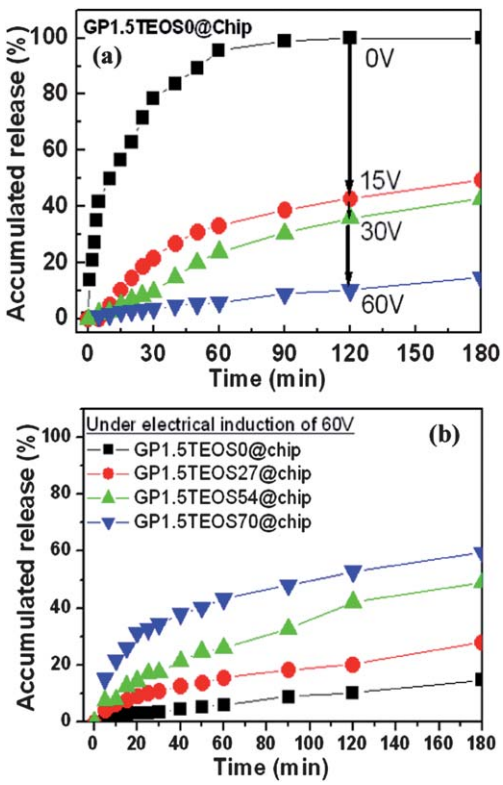

Fig. 8 (a) The ESM release profiles from GP0TEOS54 chip with applied DC voltages of 0 V, 15 V, 30 V, and 60 V, where a considerable decrease in the release amount was detected when 15 V voltage was initially applied. (b) The release profiles from the hybrid chips with different TEOS of 0%, 27%, 54%, and 70% under a DC voltage of 60 V.

The drug release rate decreased with increasing voltage. This behavior can also be explained as an interplay between the electrophoretic and electroosmosis actions aforementioned. The electrophoretic flow of ESM moved toward the anode but the electroosmotic flow carried ESM toward the cathode, the opposite and competing actions restricted drug diffusion considerably out of the chip, resulting in a slower ESM release profile.

However, under electrical stimulus, a trend similar to that of the GP effect was detected for the TEOS effect on resultant release, as illustrated in Fig. 8(b), where the ESM release turned faster with increased TEOS, which is contrary to what was detected for the hybrids without electrical stimulus, Fig. 5(b). Such a finding can be explained by the fact that the CHC polymeric network becomes less positively charged when more silica is incorporated. The action of electroosmosis is then enhanced, which further contracts the hybrid hydrogel within the chips to a certain extent under identical applied voltage, resulting in a faster ESM release rate.

Similarly, the kinetic constants (K) and diffusion exponents (n) are listed in Table 4, which are calculated according to eqn (1) from the release profiles of GP1.5TEOS0, GP1.5TEOS27, GP1.5TEOS54, and GP1.5TEOS70 chips. It was demonstrated that the exponent n was affected by the addition of TEOS, but also changed with the applied voltage. The n value decreased with increased TEOS for the case without electrical stimulus, but in the presence of applied voltage, the n value increased with increased TEOS. Under no applied voltage (0 V), the n value reduced from 0.727 to 0.451 as the TEOS increased from 0% to 70%. In this case, higher TEOS content mechanically strengthened the resulting hybrid hydrogels, rendering them more rigid and less swellable, which restricted ESM diffusion and suppressed n values, indicating the release mechanism shifted from

Table 4 Kinetic constants K, and diffusion exponents n obtained *via* linear regression of ESM release from the hybrid hydrogel chip, where the GP was fixed at 1.5%, while TEOS increased from 0% to 70% by weight

Sample label	Kinetic constant K				Release exponent n			
Applied voltage	0 V	15 V	30 V	60 V	0 V	15 V	30 V	60 V
GP1.5TEOS0	6.180	5.960	1.615	1.158	0.727	0.778	0.805	0.841
GP1.5TEOS27	5.876	5.175	2.297	1.157	0.671	0.904	0.906	0.947
GP1.5TEOS54	6.095	5.648	2.777	1.204	0.595	0.985	0.986	0.998
GP1.5TEOS70	5.402	6.114	3.864	1.953	0.451	1.001	0.989	1.103

swelling-controlled to diffusion-controlled. However, under electrical stimulus, the n value of GP1.5TEOS0 started to increase from 0.727 to 0.778 under 15 V, and then continuously increased with applied electrical voltage to $n = 0.805$ (at $E = 30$ V), and $n = 0.841$ (at $E = 60$ V). Since increased applied voltage may generate an increasing amount of negatively charged ESM, the interaction between ESM and less-positively charged CHC chains enables an increasing stretch of the CHC chains, the negatively charged TEOS along with the less-positively charged CHC enhanced the electroosmosis, which facilitated further shrinkage of hybrid hydrogels within the chip-like structure, giving rise to a swelling controlled mechanism.

On the other hand, it was also demonstrated that in the absence of applied voltage, the rate of drug release represented by the K value was decreased with increasing TEOS content. It could be explained that positively charged CHC polymer chains were interweaved with inorganic, inflexible and negatively charged silica network so that water and drug molecules had difficulty in diffusing. However, in the presence of the electric field, the action of electroosmosis is then enhanced, which further contracts the hybrid hydrogel within the chips, resulting in a faster ESM release rate because more silica can lead to a less positively charged CHC polymeric network. This result was consistent with the release profiles shown in Fig. 8(a) and (b).

Concluding remarks

A hybrid hydrogel composed of an amphiphilic chitosan and inorganic silica was assembled into a chip-like device, which was characterized in terms of its electrically modulated drug release behavior *in vitro* using an anticonvulsant drug, ethosuximide, as model molecule. The drug release behavior of the hybrid hydrogels was dependent upon the swelling of the hybrid, which has been found to be compositionally dependent in terms of the concentration of both TEOS and GP incorporated. The release behavior was explained using a combined mechanism of electrophoretic and electro-osmotic actions, which was strongly related to the electrostatic interactions among the constituting phases and drug. The hybrid hydrogel chip designed in this work has demonstrated a number of electrically modulated drug release profiles *in vitro* ranging from burst-like to slow-elution patterns. Such a drug delivery chip based on the hybrid hydrogels designed in this work provides valuable information on controlled release of ESM drug *in vitro*. A preliminary *in vivo* test in a non-implantable manner (attached to the skull of a rat model) for epileptic treatment (at a range of DC voltage of 15–60 V) had an exciting outcome where the abnormal seizure frequency can be largely reduced by ~50% with a treatment from a few to tens of minutes. The rats survived safely after the tests with no side effect detected. The work will be published elsewhere. An implantable version is currently under design with a new version of the chip.

Acknowledgements

This work was financially supported by the National Science Council of the Republic of China, Taiwan, under contracts 99-2221-E-009-070-MY3 and NSC-2113-M-009-027-MY2. This paper (work) is also supported by "Aim for the Top University Plan" of the National Chiao Tung University and Ministry of Education, Taiwan, R.O.C.

References

1 D. Shi, *Adv. Funct. Mater.*, 2009, **19**, 3356.
2 I. C. Kwon, Y. H. Bae and S. W. Kim, *Nature*, 1991, **354**, 291.
3 T. M. Allen and P. R. Cullis, *Science*, 2004, **303**, 1818.
4 M. R. Prausnitz, S. Mitragotri and R. Langer, *Nat. Rev. Drug Discovery*, 2004, **3**, 115.
5 Jindrich Kopecek, *Eur. J. Pharm. Sci.*, 2003, **20**, 1–16.
6 S. Sershen and J. West, *Adv. Drug Delivery Rev.*, 2002, **54**, 1225.
7 Y. Qiu and K. Park, *Adv. Drug Delivery Rev.*, 2001, **53**, 321.
8 J. L. Drury and D. J. Mooney, *Biomaterials*, 2003, **24**, 4337.
9 C. J. Whiting, A. M. Voice, P. D. Olmsted and T. C. B. McLeish, *J. Phys.: Condens. Matter*, 2001, **13**, 1381.
10 T. Tanaka, I. Nishio, S. T. Sun and S. Ueno-Nishio, *Science*, 1982, **218**, 467.
11 S. Ramanathan and L. H. Block, *J. Controlled Release*, 2001, **70**, 109.
12 S. H. Gehrke, *Adv. Polym. Sci.*, 1993, **110**, 81.
13 J. P. Gong, T. Nitta and Y. Osada, *J. Phys. Chem.*, 1994, **98**, 9583.
14 T. Budtova, I. Suleimenov and S. Frenkel, *Polymer*, 1995, **3**, 387.
15 S. J. Kim, S. J. Park, M.-S. Shin and S. I. Kim, *J. Appl. Polym. Sci.*, 2002, **86**, 2290.
16 S. J. Kim, S. J. Park, M.-S. Shin and S. I. Kim, *J. Appl. Polym. Sci.*, 2002, **86**, 2285.
17 S. J. Kim, S. G. Toon and S. I. Kim, *J. Polym. Sci., Part B: Polym. Phys.*, 2004, **42**, 914.
18 S. J. Kim, S. G. Toon, K. B. Lee, Y. D. Park and S. I. Kim, *Solid State Ionics*, 2003, **164**, 199.
19 T. Y. Liu, S. Y. Chen, Y. L. Lin and D. M. Liu, *Langmuir*, 2006, **22**, 9740.
20 K. H. Liu, T. Y. Liu, S. Y. Chen and D. M. Liu, *J. Nanosci. Nanotechnol.*, 2009, **9**, 1198.
21 K. H. Liu, S. Y. Chen, D. M. Liu and T. Y. Liu, *Macromolecules*, 2008, **41**, 6511.
22 S. Ramanathan and L. H. Block, *J. Controlled Release*, 2001, **70**, 109.
23 M. Lee, J. W. Nah, Y. Kwon, J. J. Koh, K. S. Lo and S. W. Kim, *Pharm. Res.*, 2001, **18**, 427.
24 T. Tanaka, *Sci. Am.*, 1981, **244**, 124.
25 J. P. Gong, T. Nitta and Y. Osada, *J. Phys. Chem.*, 1994, **98**, 9583.